

Supporting Information for:

**Room-temperature synthesis of bimetallic ZnCu-MOF-74 as adsorbent for
tetracycline removal from aqueous solution**

Catalina V. Flores,^{a,b,+} Andy Machín-Garriga,^{a,+} Juan L. Obeso,^{a,b,+} J. Gabriel Flores,^{d,e}

Ilich A. Ibarra,^{b,f} Nora S. Portillo-Vélez,^{c*} Carolina Leyva^{a*} and Ricardo A. Peralta^{c*}

^a*Instituto Politécnico Nacional, CICATA U. Legaria, Laboratorio Nacional de Ciencia, Tecnología y Gestión Integrada del Agua (LNAgua), Legaria 694, Irrigación, 11500, Miguel Hidalgo, CDMX, México.*

^b*Laboratorio de Físicoquímica y Reactividad de Superficies (LaFRoS), Instituto de Investigaciones en Materiales, Universidad Nacional Autónoma de México, Circuito Exterior s/n, CU, Coyoacán, 04510, Ciudad de México, México.*

^c*Departamento de Química, División de Ciencias Básicas e Ingeniería. Universidad Autónoma Metropolitana (UAM-I), 09340, México.*

^d*Departamento de Ingeniería de Procesos e Hidráulica División de Ciencias Básicas e Ingeniería Universidad Autónoma Metropolitana-Iztapalapa Ciudad de México, 09340, México.*

^e*Área de Química Aplicada, Departamento de Ciencias Básicas, Universidad Autónoma Metropolitana-Azcapotzalco, 02200, Ciudad de México, México.*

^f*On Sabbatical as “Catedra Dr. Douglas Hugh Everett” at Departamento de Química, Universidad Autónoma Metropolitana-Iztapalapa, Avenida San Rafael Atlixco 186, Leyes de Reforma Ira Sección, Iztapalapa, Ciudad de México 09310, México.*

⁺*These authors contributed equally to this manuscript*

Table of contents

S1. Experimental details.....S3
S2. Results and DiscussionsS7
S3. References.....S16

S1. Experimental details

Analytical instruments

Powder X-Ray Diffraction Patterns (PXRD) were recorded on a Rigaku Diffractometer, Ultima IV, with Cu-K α 1 radiation ($\lambda = 1.5406 \text{ \AA}$) using a nickel filter. The patterns were recorded in the range $2-50^\circ 2\theta$ with a step scan of 0.02° and a scan rate of $0.10^\circ \text{ min}^{-1}$. Fourier-transform infrared spectroscopy (FT-IR) spectra were obtained in the range of $4000-500 \text{ cm}^{-1}$ on a Shimadzu IRTracer-100 spectrometer using KBr pellets. Thermal gravimetric analysis (TGA) was performed using a TA Instruments Q500HR analyzer under an N_2 atmosphere using the high-resolution mode (dynamic rate TGA) at a $2^\circ\text{C}/\text{min}$ scan rate from room temperature to 640°C . Nitrogen adsorption-desorption isotherms were measured by a volumetric method using a Micromeritics ASAP 2020 gas sorption analyzer. The sample mass employed was 65.0 mg . Free space correction measurements were performed using ultra-high purity He gas (UHP grade 5, 99.999% pure). Nitrogen isotherms were measured using UHP-grade Nitrogen. All nitrogen analyses were performed using a liquid nitrogen bath at 77 K . Oil-free vacuum pumps were used to prevent contamination of sample or feed gases. The zeta potentials were measured using NanoPlus HD sizer equipment (Micrometrics, USA). Zeta potential values for the final composites were measured in a $2-9 \text{ pH}$ range. A minimum of 3 measurements per sample was done at room temperature. The variation of pH was carried out using 0.01 M NaOH and HNO_3 solutions. X-Ray Photoelectron Spectroscopy (XPS) analyses were carried out with a Thermo Scientific K-alpha X-ray photoelectron spectrometer working at 72 W and equipped with a hemispherical analyzer and a monochromatic. Survey scans were recorded using $400 \text{ }\mu\text{m}$ spot size and fixed pass energy of 200 eV , whereas high-resolution scans were collected at 20 eV of pass energy. Spectra have been charged and corrected to the mainline of the carbon $1s$ spectrum (adventitious carbon) set to 284.8 eV . Spectra were analyzed using CasaXPS software (version 2.3.14). Spectral backgrounds were subtracted using the Shirley method. Curve fitting procedures and elemental quantifications were performed with the CasaXPS program (version 2.3.14). The morphology was analyzed employing a variable pressure scanning electron microscope (SEM), brand FEI Co., and Quanta model FEG 250 with an EDS detector Bruker model XFlash 6160. The copper and nickel concentration was

measured using an Inductively Coupled Plasma Mass Spectrometer Optima 8000 (ICP-OES, Perkin Elmer, United States).

Tetracycline (TC) Adsorption Experiments.

Effect of dosage

The dosage effect was investigated for 5, 10, 15, 20, and 30 mg of ZnCu-MOF-74 with 30 mL of TC solutions (30 mg L^{-1}) for 10 h.

Influence of pH on the adsorption

Experiments were carried out in the pH range of 4-10 with 30 mL of TC (30 mg L^{-1}) solutions using 15 mg of ZnCu-MOF-74 at a specific pH value for 10 h. The pH values were adjusted using $0.1 \text{ mol L}^{-1} \text{ HNO}_3$ and NaOH. The pH measurements were conducted using a ThermoScientific pH meter.

Influence of contact time

Contact time was studied using 90 mL of TC solution (30 mg L^{-1}) with 45 mg of ZnCu-MOF-74, taking 1 mL of sample each time. The samples were analyzed at the following times 0, 5, 7, 15, 30, 60, 90, 120, 180, 240, 360, 480, and 600 min.

Influence of initial concentration

The initial concentration experiments were conducted at room temperature for 10 h using ZnCu-MOF-74 with different TC concentrations (30, 40, 60, 80, 100, 200 and 300 mg L^{-1}) with 15 mg of ZnCu-MOF-74 in 30 mL.

Reusability

The reusability of ZnCu-MOF-74 was tested for four adsorption-desorption cycles using methanol as desorbing agent for 10 h, respectively.

Effect of temperature

For evaluating the effect of temperature, 30 mL of TC solution (30 mg L^{-1}) with 15 mg of ZnCu-MOF-74 was varied on three points (25, 40 and $60 \text{ }^\circ\text{C}$) with a TC initial concentration (30 mg L^{-1}). The Van't Hoff equation (Eq. (1)) was used to estimate the thermodynamic parameters. The change in free energy (ΔG°), change in enthalpy (ΔH°),

and change in entropy (ΔS°) were calculated using Eq. 1 and 2. Where K_c (Eq. (3)) is the equilibrium constant, R (8.314 Jmol⁻¹K⁻¹) is the gas constant, and T (K) is the adsorption temperature.

$$\ln(K_c) = \frac{\Delta S^\circ}{R} - \frac{\Delta H^\circ}{RT} \quad (1)$$

$$\Delta G^\circ = \Delta H^\circ - T\Delta S^\circ \quad (2)$$

$$K_c = \frac{Q_e}{C_e} \quad (3)$$

Kinetic adsorption experiments

Table S1. Kinetics models for the TC adsorption		
Kinetic model	Non-linear equation	Parameter
PFO model	$q_t = q_e(1 - e^{-k_{p1}t})$	q_e : adsorption capacities at equilibrium (mg g ⁻¹); q_t : adsorption capacities at time t (mg g ⁻¹); k_{p1} : pseudo-first-order rate constant for the kinetic model (mg g ⁻¹ min).
PSO model	$q_t = \frac{k_{p2}q_e^2t}{1 + k_{p2}q_e t}$ $h = k_{p2} \times q_e^2$	q_e : adsorption capacities at equilibrium (mg g ⁻¹); q_t : adsorption capacities at time t (mg g ⁻¹); k_{p2} : pseudo-second-order rate constant of adsorption (mg g ⁻¹ min); h : initial adsorption rate (mg g ⁻¹ min ⁻¹).
Elovich model	$q_t = \frac{1}{\beta} \ln(1 + \alpha\beta t)$	q_t : adsorption capacities at time t (mg g ⁻¹); α : adsorption equilibrium constant (mg g ⁻¹ min ⁻¹); β : equilibrium constant desorption (g mg ⁻¹).
IPD model	$q_t = K_{ip}t^{0.5} + C_i$	q_t : adsorption capacities at time t (mg g ⁻¹); K_{ip} : rate parameter of stage i (mg g ⁻¹ min ^{-1/2}); C_i :

		intercept of stage i that gives an idea about of the thickness of boundary layer (mg g^{-1}).
--	--	--

Adsorption isotherms experiments

Table S2. Adsorption isotherm equations and parameters		
Isotherm	Non-linear equation	Parameter
Langmuir	$Q_e = \frac{Q_m K_L C_e}{1 + K_L C_e}$ $R_L = \frac{1}{1 + K_L C_o}$ $\Delta G(\text{kJ/mol}) = -RT \ln K_o$ $K_o = K_L * MM * 10^3$	Q_m is maximum adsorption capacity (mg g^{-1}); Q_e : amount of adsorbate in the adsorbent at equilibrium (mg g^{-1}); K_L is adsorption intensity or Langmuir coefficient (L mg^{-1}); R_L is separation factor; ΔG free Gibbs energy (kJ mol^{-1}). MM: Molar mass (g mol^{-1})
Freundlich	$Q_e = K_F C_e^{1/n}$	K_F is the constant indicative of the relative adsorption capacity (L g^{-1}) and n is indicative of the intensity
Temkin	$Q_e = \frac{RT}{bt} * \ln(At * Ce)$ $B = \frac{RT}{bt}$	At : Temkin isotherm equilibrium binding constant (L g^{-1}); bt : Temkin isotherm constant; R : universal gas constant ($8.314 \text{ J mol}^{-1} \text{ K}^{-1}$); T : Temperature at 298 K; B : Constant related to heat of sorption (J mol^{-1})

S2. Results and Discussions

Synthesis of ZnCu-MOF-74

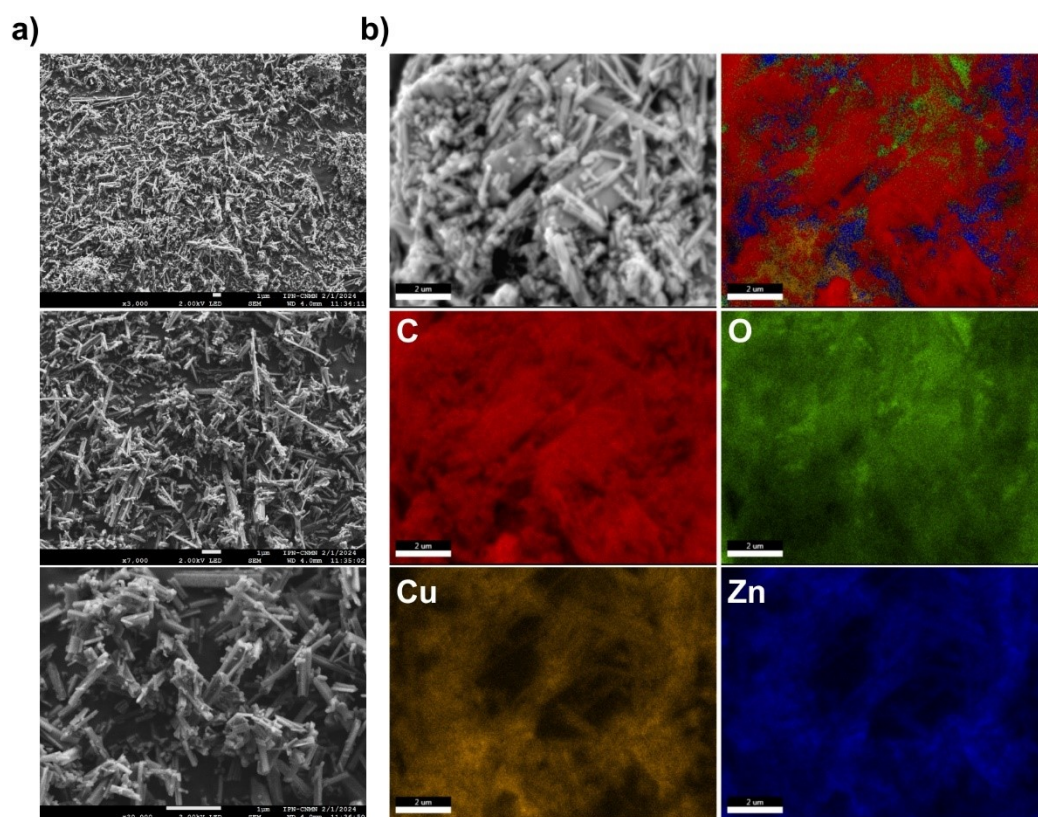


Figure S1. a) Detailed SEM-micrographs and b) elemental map distribution of ZnCu-MOF-74.

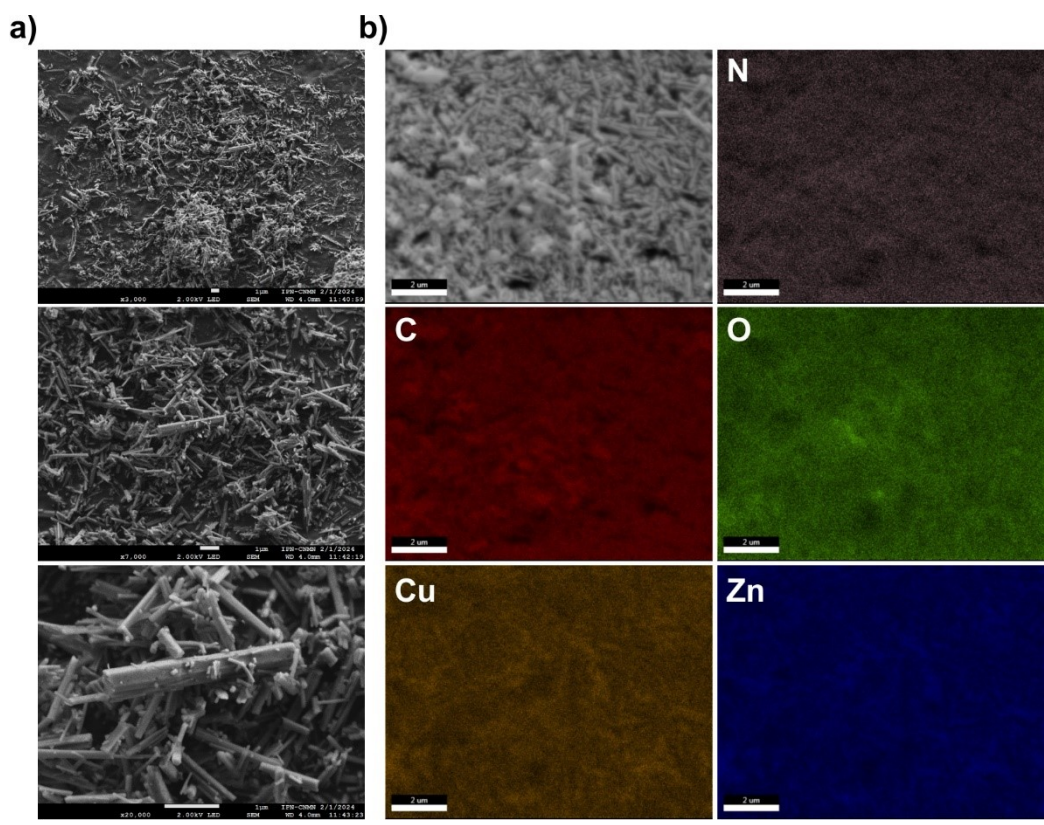


Figure S2. a) Detailed SEM-micrographs and b) elemental map distribution of ZnCu-MOF-74 after TC adsorption.

Tetracycline (TC) structure

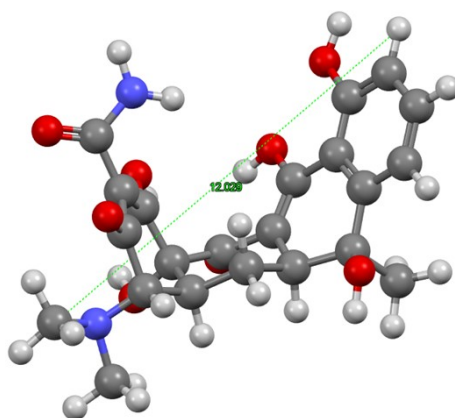


Figure S3. The structure of TC. Atoms label: grey: carbon, white: hydrogen, red: oxygen, and blue: nitrogen.

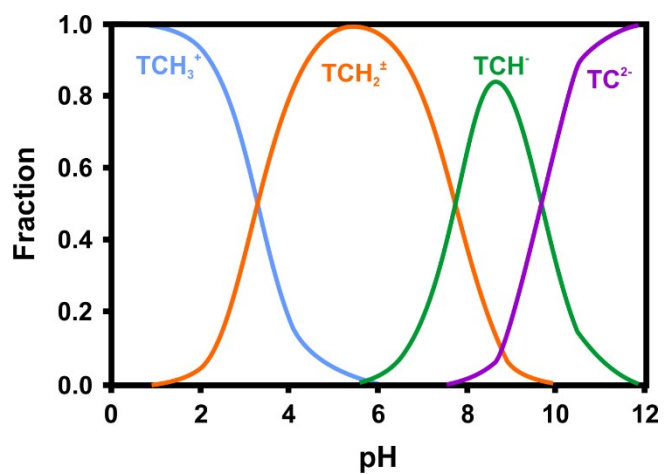
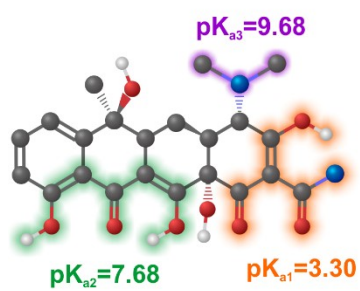


Figure S4. The speciation structure of TC.

Table S3. Comparison of the Langmuir maximum adsorption capacity of ZnCu-MOF-74 with the MOF-based adsorbents, common and commercial materials reported.						
MOF-Based Sorbent	pH	Time (h)	q_e mg g⁻¹	BET m² g⁻¹	Interaction	Ref
MOF-5	6	0.75	233	2510	π - π interactions	1
MOF-525/GO	3	6	436	444	π - π stacking and hydrogen bonding, complexation	2
PCN-128Y			423		complexation	3
MIL-68(Al)/GO	8	12	228	1266	π - π stacking and hydrogen bonding, Al-N covalent bonding	4
UiO-66	7	0.66	145	1249	π - π stacking cation- π	5
NU-1000	7	0.6	356	1487		
MOF-525	5	2	807	2224		
MOF-818	3		442	1408	π - π interaction	6
Ni/Co-MOF@CMC	6	0.08	624		chemisorption	7
MIL-101(Fe)	8	5	420	982	π - π interaction, hydrogen bond, coordinate bonds, pore filling, electrostatic interactions	8
MIL-88A(Fe)		10	379	231		
MIL-53(Fe)		10	254	21		
Zr-MOF-20	10	9	196	337	π - π interaction, hydrogen bond, pore/size-selective adsorption	9
ZnCu-MOF-74	6	6	775	1142		This work

Kinetic adsorption experiments

Table S4. Parameters of the kinetic models.		
Model	Parameter	Material
		ZnCu-MOF-74
PFO model	q_e ($mg\ g^{-1}$)	51.97
	K_1 ($mg\ g^{-1}\ min^{-1}$)	0.17
	R^2	0.682
PSO model	q_e ($mg\ g^{-1}$)	54.22
	K_2 ($mg\ g^{-1}\ min^{-1}$)	0.005
	h	15.20
	R^2	0.904
Elovich model	β ($mg\ g^{-1}$)	0.216
	α ($mg\ g^{-1}\ min^{-1}$)	2295.61
	R^2	0.957
IPD model	K_{ip} ($mg\ g^{-1}\ min^{-1}$)	0.885
	C_i ($mg\ g^{-1}$)	38.60
	R^2	0.765

Adsorption isotherms

Table S5. Parameters of the isotherm's models.		
Model	Parameter	Material
		ZnCu-MOF-74
Freundlich	K_F ($L\ g^{-1}$)	44.12
	n	1.60
	χ^2	365.23
	R^2	0.989
Langmuir	Q_m ($mg\ g^{-1}$)	775.66
	K_L ($L\ mg^{-1}$)	0.034

	R_L	0.49-0.08
	$\Delta G(kJ mol^{-1})$	-18.13
	χ^2	331.53
	R^2	0.990
	Temkin	
	$A_t(L g^{-1})$	0.433
	b_t	16.78
	$B(J mol^{-1})$	0.147
	χ^2	1164.0
	R^2	0.927

Parameters of the thermodynamic experiments

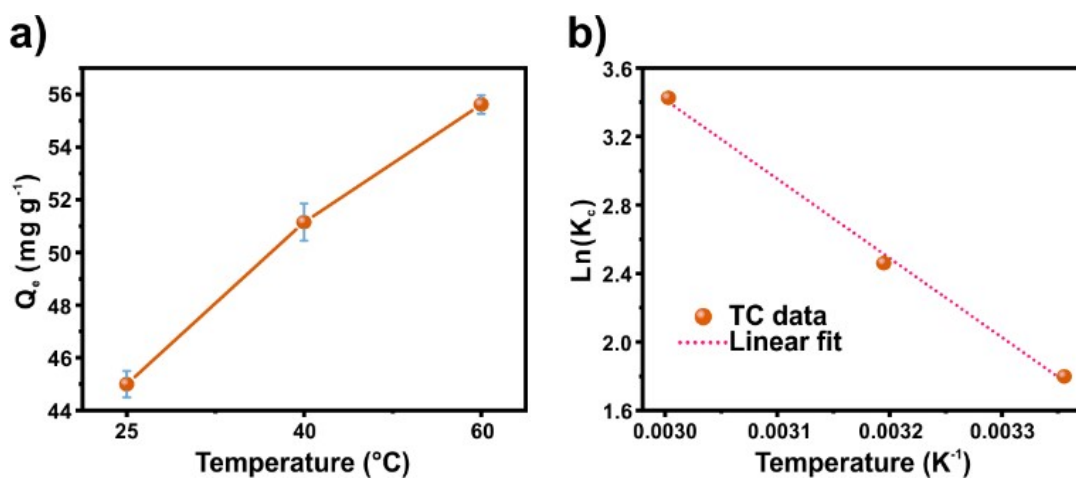


Figure S5. a) Temperature variation effect [15 mg, 30 ml, 30 mg L⁻¹, 6.5 pH, 1 h]; and b) thermodynamic fit.

Material	T (K)	Function			
		ΔS° (kJ mol ⁻¹ K ⁻¹)	ΔH° (kJ mol ⁻¹)	ΔG° (kJ mol ⁻¹)	R^2
ZnCu-MOF-74	298	0.144	38.45	-4.38	0.997
	313			-6.54	
	333			-9.42	

PXRD and FT-IR after ads/des cycles.

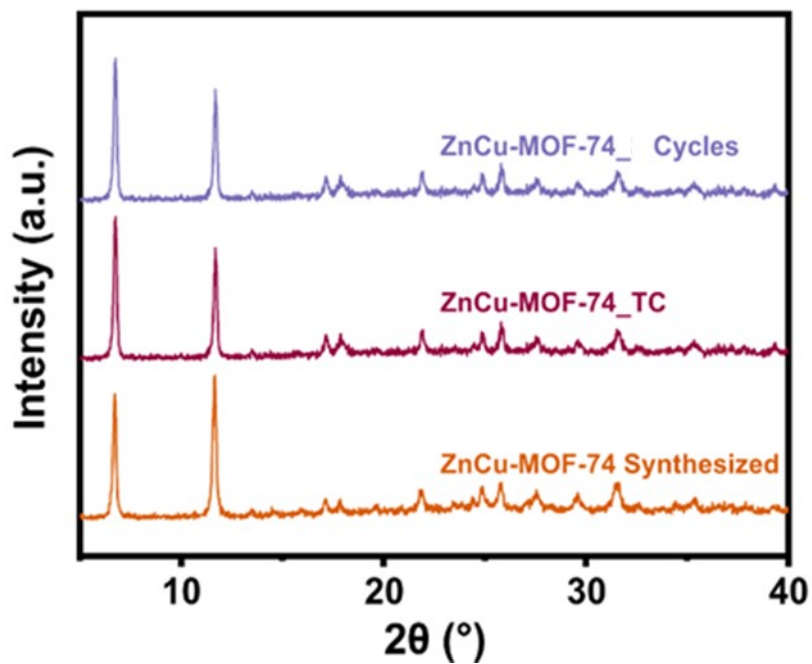


Figure S6. PXRD patterns of ZnCu-MOF-74 after the adsorption and cyclability process.

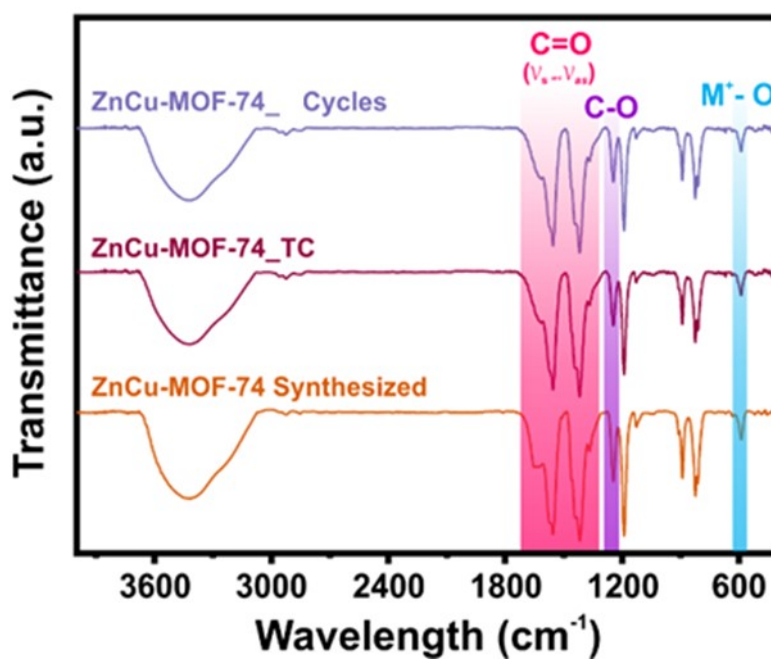


Figure S7. FTIR spectra of ZnCu-MOF-74 after the adsorption and cyclability process.

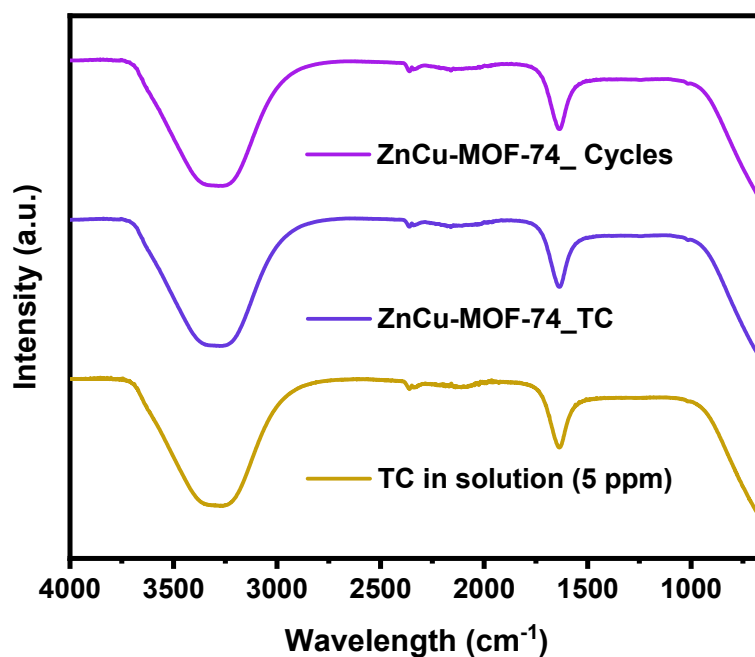


Figure S8. FTIR spectra in the liquid phase of the remaining water solution after the adsorption and cyclability process.

XPS

Table S7. XPS survey data (atomic percentage) of the different elements in ZnCu-MOF-74.					
Samples	Elements (At. %)				
	C 1s	O 1s	Zn 2p	Cu 2p	N 1s
ZnCu-MOF-74	61.6	30.2	4.0	2.9	-
ZnCu-MOF-74_TC	69.4	24.8	0.7	1.7	3.3

Table S8. The peak-fitting results of C 1s high-resolution signal of ZnCu-MOF-74.				
Samples	Assignment	E_B (eV)	FWHM (eV)	At. %
ZnCu-MOF-74	C1s _{C=C aromatic}	284.4	1.7	54.2
	C1s _{C-OH}	285.8	1.8	23.4
	C1s _{O-C=O}	288.4	1.9	17.6
	C1s _{π-π^*}	290.1	2.0	4.8
ZnCu-MOF-	C1s _{C=C aromatic}	284.3	1.7	60.4

74_TC	C1s C-OH	285.9	1.8	25.4
	C1s O-C=O	288.0	1.9	11.4
	C1s π - π^*	290.0	2.0	2.8

Table S9. The peak-fitting results of O 1s high-resolution signal of ZnCu-MOF-74.

Samples	Assignment	E _B (eV)	FWHM (eV)	At. %
ZnCu-MOF-74	O 1s Cu-O, C=O	531.1	1.5	33.5
	O 1s C-OH	532.0	1.5	49.1
	O 1s H ₂ O	533.4	1.6	77.4
ZnCu-MOF-74_TC	O 1s Cu-O, C=O	530.6	1.5	25.4
	O 1s C-OH	531.6	1.5	48.4
	O 1s H ₂ O	533.0	1.6	26.2

Table S10. The peak-fitting results of Cu 2p_{3/2} high-resolution signal of ZnCu-MOF-74.

Samples	Assignment	E _B (eV)	FWHM (eV)	At. %
ZnCu-MOF-74	Cu 2p_{3/2} Cu ⁺	933.2	2.0	23.8
	Cu 2p_{3/2} Cu ²⁺	935.0	2.2	76.2
	Satellite Cu ²⁺	939.5	4	-
	Satellite Cu ²⁺	943.9	3.8	-
ZnCu-MOF-74_TC	Cu 2p_{3/2} Cu ⁺	932.6	2.0	21.9
	Cu 2p_{3/2} Cu ²⁺	934.4	2.2	78.1
	Satellite Cu ²⁺	938.8	4.0	-
	Satellite Cu ²⁺	943.5	3.6	-

Table S11. The peak-fitting results of Zn 2p high-resolution signal of ZnCu-MOF-74.

Samples	Assignment	E _B (eV)	FWHM (eV)	At. %
ZnCu-MOF-74	Zn 2p_{3/2}	1022.2	2.2	67
	Zn 2p_{1/2}	1044.8	2.3	33
ZnCu-MOF-	Zn 2p_{3/2}	1021.7	2.2	65.1

74_TC	Zn 2p _{1/2}	1044.8	2.3	35.9
-------	----------------------	--------	-----	------

S3. References

- 1 S. M. Mirsoleimani-azizi, P. Setoodeh, S. Zeinali and M. R. Rahimpour, *Journal of Environmental Chemical Engineering*, 2018, **6**, 6118–6130.
- 2 B. Chen, Y. Li, M. Li, M. Cui, W. Xu, L. Li, Y. Sun, M. Wang, Y. Zhang and K. Chen, *Microporous and Mesoporous Materials*, 2021, **328**, 111457.
- 3 Y. Zhou, Q. Yang, D. Zhang, N. Gan, Q. Li and J. Cuan, *Sensors and Actuators B: Chemical*, 2018, **262**, 137–143.
- 4 L. Yu, W. Cao, S. Wu, C. Yang and J. Cheng, *Ecotoxicology and Environmental Safety*, 2018, **164**, 289–296.
- 5 J. Xia, Y. Gao and G. Yu, *Journal of Colloid and Interface Science*, 2021, **590**, 495–505.
- 6 Z. Zhang, C. Ding, Y. Li, H. Ke and G. Cheng, *SN Appl. Sci.*, 2020, **2**, 669.
- 7 W. Yang, Y. Han, C. Li, L. Zhu, L. Shi, W. Tang, J. Wang, T. Yue and Z. Li, *Chemical Engineering Journal*, 2019, **375**, 122076.
- 8 Z. Zhang, Y. Chen, Z. Wang, C. Hu, D. Ma, W. Chen and T. Ao, *Applied Surface Science*, 2021, **542**, 148662.
- 9 J. Zhong, X. Yuan, J. Xiong, X. Wu and W. Lou, *Environmental Research*, 2023, **226**, 115633.